A Comparison Model for WLAN Technologies, 802.11n and HeNB in LTE and the Future 5G Networks

Kuo-Chang Ting

Dept. of Business Administration and Dept. of Information Engineering Taiwan Minghsin University of Science and Technology, Taiwan
ting@must.edu.tw

Abstract

The fifth generation (5G) mobile communication technologies are expected to attain 1000 times higher mobile data volume per unit area, 10 to 100 times higher number of connected devices and user data rate, 10 times longer battery life and 5 times shorter latency. Home eNodeB (HeNB) (also known as Femtocell Access Point, FAP) and 802.11n WLAN are promising technologies to attain the goals set above, particularly for indoor connections because of the short distance connection characteristics for WLAN. The comparison and analysis between these two technologies based on PHY data rate, MAC layer throughput and power consumption are essential for users to make the right choice. Our contributions mainly fall on that the models established in this article are helpful to develop the next generation of small cell technology and WLAN for the future 5G networks including the recent development, LTE operated on unlicensed bands. Furthermore, an interference model of HeNB and 802.11n is also analyzed. To our knowledge, this study is not much addressed in other works so far.

Keywords: 5G, 802.11n, 802.11ac, HeNB, LTE, LTE-U, LAA, Throughput

1 Introduction and Related Works

The evolving fourth-generation (4G) wireless technologies, such as long term evolution (LTE) of Universal Mobile Telecommunications System (UMTS) [1] and Worldwide Interoperability for Microwave Access (WiMAX) offer wider bandwidth for high data rates. These high data rates over the access part of the network are achieved through the deployment of higher order modulation, such as 64-quadrature amplitude modulation (QAM), advanced coding techniques, convolutional turbo codes combined with advanced antenna techniques, such as space-division multiple access (SDMA) [2], multiple-input multiple-output (MIMO) [3], and so on. The applications of cloud computing, software as a service (SaaS), platform as a service (PaaS), and infrastructure as a service (IaaS) will prevail in the future, and more and more mobile devices will connect to the Internet any time and any place. Hence, LTE and LTE-A cannot meet this demand in the near future and the traffic congestion problem will be inevitable due to the spectrum limitation. Frequency reuse might be the most promising technique to increase the total capacity of a cell for the future 5G networks. Moreover, once a user equipment (UE) enters a building, the data rate will drop sharply due to the large path loss, especially if the building is made up of concrete walls. In general, the path loss can be up to 15 to 20 dB [4]. The UE can even lose their connectivity to the evolved Node B (eNB) due to this large path loss. The eNB in LTE networks or the future 5G networks must allocate more resource blocks to the UEs to maintain the same data rate under the low signal-to-noise ratio (SNR) environment. This aggravates the problem of insufficient frequency spectrum.

The energy consumption of UE while connecting to the eNB is very high due to the long distance between UE and eNB in general. Furthermore, about 80% of connections of an eNB are established in indoor environments according to the statistics [5]. This expedites the emergence and development of the new generation of WLAN technologies such as 802.11n and 802.11ac and small cell base station technologies such as microcell and Home eNodeB (HeNB) in LTE networks. HeNB also called Femtocell is a technology to solve the problem of limited frequency spectrum and high path loss in indoor environments for the LTE and the future 5G networks. The operation of a HeNB illustrated in Figure 1 shows that one or more UEs may connect to the Internet via the relay of a HeNB to the broadband router of operators. The access technology for the HeNB is identical to the eNB so that UE can easily perform hand-off between eNB and HeNB while maintaining continuous communication with the operator network. Modern smart phones usually support both 802.11 and LTE or the future 5G network connections, making the decision on which technology to use for connecting to the Internet a critical and interesting issue regardless of the proposal of the inter-networking

*Corresponding Author: Kuo-Chang Ting; E-mail: ting@must.edu.tw
DOI: 10.3966/160792642018011901025

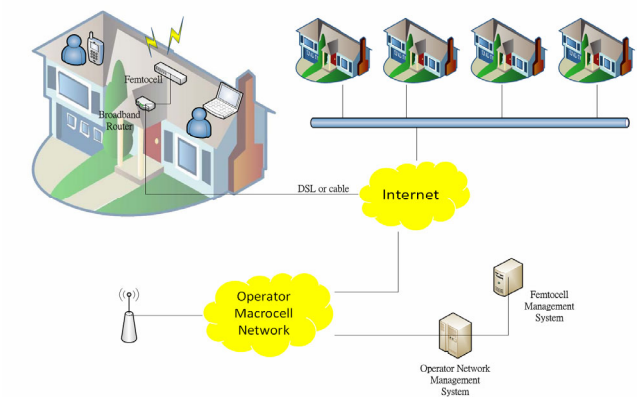

Figure 1. Illustration of HeNB operation

between WLAN and 3GPP having proposed about one decade ago [6]. Note that the interference of HeNB networks has been studied in [7-11], but a model to evaluate the capacity of HeNB and 802.11n with or without interference is rarely addressed in the previous works so far. In this paper, we construct a model to evaluate the throughput of the WLAN technologies in PHY and MAC layers. Next, we take interference into account for the Access Point (AP) in 802.11n and HeNB in LTE networks. It is especially challenging for the HeNB to solve the problem of co-tier and cross-tier co-channel interference. In the remainder of this paper, we analyze the PHY throughput and spectral efficiency of 802.11n and HeNB in Section 2. An analysis model to evaluate the throughput of 802.11n and HeNB in MAC is established in Section 3. An interference model for HeNB is described in Section 4. Discussions and comparisons of 802.11n and HeNB are given in Section 5. A brief comparison between 802.11ac and HeNB for the future 5G networks is also discussed in this section. Conclusions and future works are given in Section 6.

2 The Throughput of 802.11n and HeNB in PHY Layer

2.1 The PHY Data Rate without Considering the Overheads

The throughput of 802.11n and HeNB in PHY layer can be evaluated by the same model based on the Orthogonal Frequency-Division Multiplexing (OFDM) scheme if we ignore their PHY and MAC overheads. Consider a UE with MIMO capability. Regardless of the category of the UE, if we consider the cyclic prefix (CP) T_{CP} as factor, the throughput of the OFDM system in PHY can be modeled as

$$PHY(T_{CP}) = N_{SS} \times \frac{N_{BPSC} \times r_c \times N_{SC}}{(T_{CP} + T_{SYM})} \quad \textbf{(1)}$$

where N_{SS}, N_{BPSC}, r_c, N_{SC}, T_{CP} and T_{SYM} denote the number of spatial streams, the number of bits per subcarrier, the coding rate, the number of subcarriers, the length of cyclic prefix (CP) and the symbol time, respectively. Note that the T_{CP} for the 802.11n is fixed to 0.4μs or 0.8μs depending on the modulation scheme. If the modulation scheme is fixed, the cyclic prefix time is fixed. In fact the PHY of HeNB in LTE networks based on the Orthogonal Frequency Division Multiple Access (OFDMA) is very similar to the OFDM used in 802.11n and 802.11ac. Hence, the throughput of HeNB can also be calculated by (1) if the cyclic prefix time for each symbol is fixed. However, the PHY throughput is determined by the throughput of a slot time consisting of 7 symbol time, and the CP used to avoid the inter-symbol interference (ISI) is variable for these seven symbols as mentioned in the latter section. For the normal cyclic prefix in LTE-FDD, the CP of the first symbol is 5.2 μs called long cyclic while the remaining symbol time can be as short as 4.7 us called short cyclic prefix. As a result, the PHY throughput of LTE can be calculated based on (1) with the seven symbols with 1 long or 6 short CPs; so the average throughput of HeNB T_{HeNB} can be obtained by

$$T_{HeNB} = \frac{PHY(L_{CP}) + (N_{Slot}^{Symbol} - 1)PHY(S_{CP})}{N_{Slot}^{Symbol}} \quad \textbf{(2)}$$

where N_{Slot}^{Symbol}, L_{CP} and S_{CP} denote the number of symbols per slot, the length of the long CP and the length of the short CP, respectively. If the parameters for 802.11n and HeNB in LTE FDD networks are given in Table 1, the throughput in PHY and the spectral efficiency without considering overheads are shown in Figure 2(a) and Figure 2(b) respectively based on (1) and (2). Note that our model can also be applied to LTE TDD and the performance is similar. In fact, if a UE of HeNB in LTE networks is only equipped with one antenna instead of 4 assumed in Table 1 due to the limited size of the UE generally, the number of spatial streams, N_{SS} will be reduced from 4 to 1. Therefore, the uplink data rate is reduced to one-fourth of the peak data rate, about 93.3 Mbps; as a result, its spectral efficiency is also reduced to 4.66 bps/Hz about one-fourth of the peak spatial efficiency.

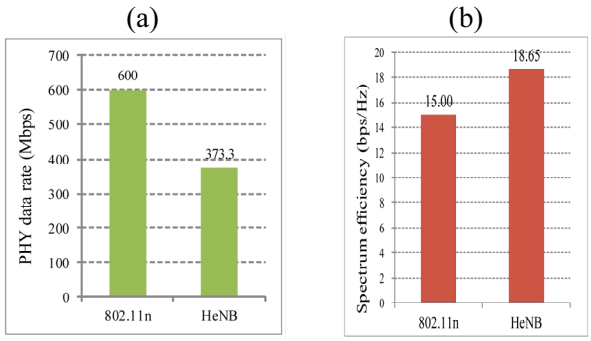

Figure 2. (a) A comparison of PHY data rate for 802.11n and HeNB; (b) A comparison of spectrum efficiency for 802.11n and HeNB

Table 1. The parameters of 802.11n and HeNB in LTE FDD networks

Symbol	802.11n	HeNB
N_{SS}	4 (4×4 MIMO)	4 (4×4 MIMO)
N_{BPSC}	6 (64QAM)	6 (64QAM)
r_c	5/6 (MCS index =31)	948/1024 (CQI=15)
N_{SC}	108 (40 MHz)	1200 (20 MHz, 100 PRB)
T_{CP}	0.4 μs	5.2 μs (L_{CP}) for the first symbol and 4.7 μs (S_{CP}) for the remaining symbols
T_{SYM}	3.2 μs	66.65 μs ((500-5.2-6×4.7)/7)

2.2 The PHY Data Rate with Overheads

In order to synchronize the sender and receiver for Single-Input Single-Output (SISO) or MIMO, the reference signal (RS) overhead in PHY layer is inevitable for both 802.11n and HeNB, the percentage of the overhead is around (2/3)/14 ≈ 4.7% for HeNB [12-13] because the RSs for SISO take 2 symbols per sub-frame for every three resource elements. So, the maximal throughput for SISO is around 93.3×(100%−4.7%) ≈ 88.9. If 4×4 MIMO is used for HeNB, the number of spatial streams is 4, but the overheads of reference signals are higher compared to SISO. The percentage of these overheads is (6/3)/14 ≈ 14.28% for each spatial stream. Each spatial stream must take 6 symbols per sub-frame for every three resource elements to distinguish from one another. Thus, the maximal throughput for downlink is around 373×(100−14.28)% ≈ 319.95 Mbps. The spectral efficiency of HeNB downlink in LTE networks is reduced to around 16. For the uplink throughput of HeNB, the RSs in PHY are located in the middle symbol of a slot time, so the percentage of RS overhead in the uplink is around 1/7. This is mixed with that of MAC layer. Thus, we do not consider it in this subsection. The PHY overhead of 802.11n depends on the format of Physical Layer Convergence Protocol (PLCP) Protocol Data Unit (PPDU) whose format is shown in Figure 3 [14].

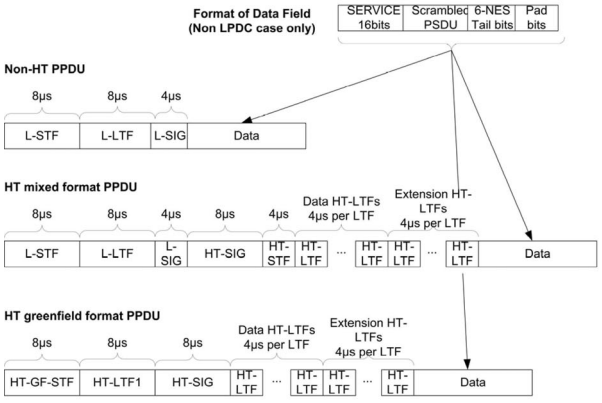

Figure 3. The PPDU formats of 802.11n

Figure 3 shows that the PHY overhead of High Throughput (HT) formats such as HT mixed and HT greenfield is higher than that of non-HT PPDU, but the PPDU format of non-HT does not have MIMO capability. In this article, we select the HT mixed format PPDU based on practical considerations because this format is compatible with the legacy 802.11a/g. So far, the new generation of 802.11, the 802.11ac has selected this format as a default setting. The percentage of overhead O for the HT mixed format PPDU can be obtained by

$$O = \frac{H}{S_{PPDU} \times 8/(R_b) + H} \quad \textbf{(3)}$$

where H, S_{PPDU} and R_b denote the aggregated duration of PPDU header and RS for synchronization in seconds, the size of PLCP Service Data Unit (PSDU) in bytes and PHY data rate in bits per second, respectively. The PSDU size can be up to 64 Kbytes using frame aggregation and the overhead can be minimized in this scenario. On the contrary, if the size of PSDU is small, the overhead will be high. The data rate R_b also impacts this overhead. As shown in (3), higher R_b results in larger percentage of overhead. Figure 3 also shows that the overhead is around 40, 48, and 64 μs for SISO, 2×2 MIMO and 4×4 MIMO, respectively. Therefore, the percentage of overhead is around 6.8% for 4×4 MIMO when S_{PPDU} is 64 KB and R_b and spectral efficiency of 802.11n reduce to 559 Mbps and 13.98 bps/Hz, respectively. If we combine (1), (2) and (3), the throughput with RSs and the percentage of overhead for HeNB, 802.11n with 1.5 KB PPDU and 802.11n with 64 KB PPDU are shown in Figure 4. Figure 4 shows that the percentage of RS overhead for 802.11n with 64 KB PPDU (6.8%) is very low compared to that for HeNB (14.3% for 4×4 MIMO). However, if the size of PPDU is reduced to 1.5 KB, the maximal size of a normal Ethernet frame, the percentage of RS overhead can be as high as 76.2%. The throughput of 802.11n with 1.5 KB PPDU shows no sharp difference among the SISO, 2×2 MIMO and 4×4 MIMO cases. The percentage of RS overhead for the 4×4 MIMO is always the largest compared to those of SISO and 2×2 MIMO because 4×4 MIMO has the highest data rate among the three schemes.

3 The Throughput of HeNB and 802.11n in MAC Layer

3.1 The MAC throughput of HeNB in LTE Networks

The multiple access technique used in LTE networks is based on OFDMA for downlink transmission which is somewhat different from the OFDM used in 802.11n. OFDMA allows many UEs to access the channel simultaneously using FDMA as in 3GPP LTE FDD

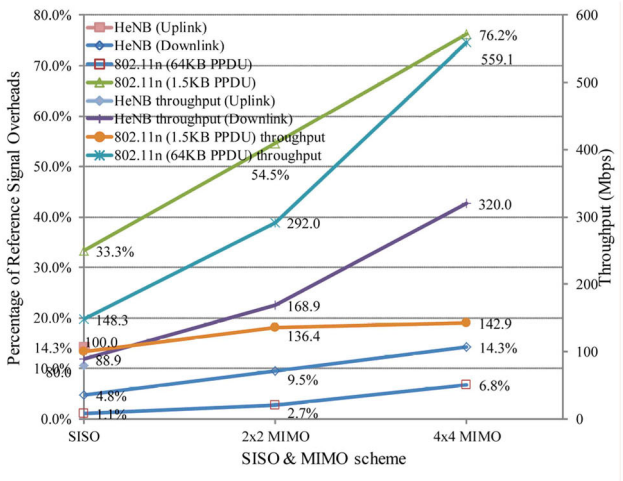

Figure 4. Percentage of RS overhead and the throughput with RS for 802.11n and HeNB in PHY

networks. User data in the downlink is carried in the physical downlink shared channel (PDSCH). The 1 ms resource allocation interval for downlink is the same as that for uplink. Resource is allocated in units of 12 sub-carriers called a resource block (RB). The eNB carries out RB allocation based on the channel quality indicator (CQI) reported by UEs. RBs are allocated in both time domain and frequency domain. The physical downlink control channel (PDCCH) is used to inform a UE of the RBs allocated for it. The data in PDSCH occupy 3 to 6 symbols in each 0.5 ms slot depending on the allocation for PDCCH and whether a normal or extended CP is used. Within a 1 ms sub-frame, only the first slot contains PDCCH while the second slot is purely for data (PDSCH). For an extended CP, 6 symbols are accommodated in a 0.5 ms slot, while for a normal CP, 7 symbols can be fitted. Normal CP is selected for the channel in the HeNB due to the short distance between the UE and HeNB. The example in Figure 5 [13] assumes 3 symbols for PDCCH but this can vary from 1 to 3.

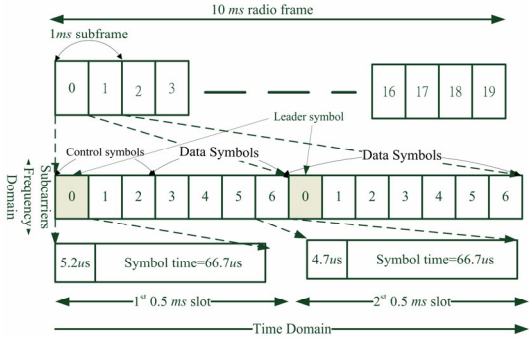

Figure 5. Downlink slot structure for bandwidths above 1.4 MHz

The uplink throughput of a UE of category 5 is much lower than that of the downlink. The uplink overhead, as reflected in physical uplink control channel (PUCCH), includes CQI, RS, ACK/NAK, scheduling request and other control information. Thus, the peak data rate of the uplink is approximately one-fourth of downlink capacity due to the one-antenna configuration. The downlink overheads, as reflected in PDCCH, include traffic indication, grants on resource assignment, ACK/NAK and other control information. The evaluation of MAC throughput in HeNB is much harder than that in 802.11n because its exact data rate depends on the implementation of resource control. We model the downlink and uplink MAC throughput of HeNB by

$$MAC_D = PHY_D \times (1 - \frac{N_{PDCCH} + N_O}{N_{Total}}) = PHY_D \times (1 - \frac{N_{PDCCH} + N_O}{N_{RB} N_{RB}^{Symbol} N_{Symbol}^{Sub}}) \quad \textbf{(4)}$$

and

$$MAC_U = PHY_U \times (1 - \frac{N_{PUCCH}}{N_{Total}}) = PHY_U \times (1 - \frac{N_{PUCCH}}{N_{RB} N_{RB}^{Symbol} N_{Symbol}^{Sub}}) \quad \textbf{(5)}$$

where PHY_D and PHY_U denote the data rate of HeNB networks in downlink and uplink with PHY overhead, respectively. N_{Total}, N_{PDCCH} and N_{PUCCH} denote the number of total resource elements, and the number of resource elements used in transferring control information for the PDCCH and PUCCH, respectively. The number of total resource elements N_{total} can be derived by multiplying the number of RBs N_{RB} by the number of subcarriers per symbol N_{Symbol}^{Sub} and the number of symbols per RB N_{RB}^{Symbol}. Note that N_O in (4) denotes the number of resource elements used in sending the information carried by Physical Broadcast Channel (PBCH), Physical Control Format Indicator Channel (PCFICH) and one group of Physical Hybrid Automatic Repeat Request Indicator Channel (PHICH). These overheads are located on the outmost RB of the allocated bandwidth for the UE. Hence, the overhead depends on the bandwidth ranging from below 1% at 20 MHz to approximately 9% at 1.4 MHz [13]. The precise estimation is also dependent on how often the control signal is transmitted. In this capacity estimation, this overhead is set to around 1%, where N_{PUCCH}=2×1/2× $N_{Symbol}^{Sub} N_{RB}^{Symbol}$ and N_{RB}=100. If the number of UEs using the same frame time increases, the number of allocated RBs decreases resulting in larger overheads. Note that the overheads in the retransmission of transmission blocks in MAC HARQ and RLC ARQ are ignored in (4) and (5). If we take the error ratio into consideration, the MAC throughput of downlink and uplink can be obtained by

$$MAC_D^e = PHY_D \times (1 - \frac{N_{PDCCH} + N_o}{N_{RB} N_{Symbol}^{Sub} N_{RB}^{Symbol}}) \left\{ \frac{1}{\sum_{i=1}^{M_C} (i) \times e^{i-1} (1-e)} \right\}$$

$$= PHY_D \times (1 - \frac{N_{PDCCH}}{N_{RB} N_{Symbol}^{Sub} N_{RB}^{Symbol}}) \left\{ \frac{1-e}{1-(M_C+1-eM_C)e^{M_C}} \right\} \quad (6)$$

and

$$MAC_U^e = PHY_U \times (1 - \frac{N_{PUCCH}}{N_{RB} N_{Symbol}^{Sub} N_{RB}^{Symbol}}) \left\{ \frac{1}{\sum_{i=1}^{M_C} (i) \times e^{i-1} (1-e)} \right\}$$

$$= PHY_U \times (1 - \frac{N_{PUCCH}}{N_{RB} N_{Symbol}^{Sub} N_{RB}^{Symbol}}) \left\{ \frac{1-e}{1-(M_C+1-eM_C)e^{M_C}} \right\}. \quad (7)$$

Here, M_C denotes the maximal times of re-transmission. In fact, the error rate e in (6) and (7) is closely related to the received SINR of a receiver and the overheads of ACK/NAK are functions of the error rate. The downlink MAC throughput of HeNB without error and with a 10% block error rate is shown in Figure 6 and Figure 7, respectively. If we let M_C be infinite in (6) and (7), the part of e^{M_C} in (6) and (7) approaches 0, so e^{M_C} can be ignored if e is not too large. Note that the overhead of PUCCH is fixed to one symbol per slot time if RS overhead is considered. Moreover, the throughput evaluation is based on the throughput in PHY layer given by (2). The gap of peak throughput between PHY (320 Mbps) and MAC (294 Mbps) layers is approximately 26 Mbps for 4×4 MIMO in HeNB, as shown in Figure 4 and Figure 6. On the contrary, the gap of peak throughput between PHY and MAC layers in 802.11n can be as large as 84.8 Mbps shown in the latter subsection. In summary, the distributed and easy approach adopted in the MAC of 802.11 pays the penalty of performance loss.

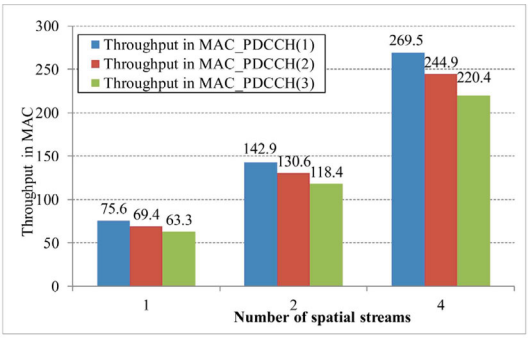

Figure 6. The downlink throughput of HeNB in MAC with a perfect channel

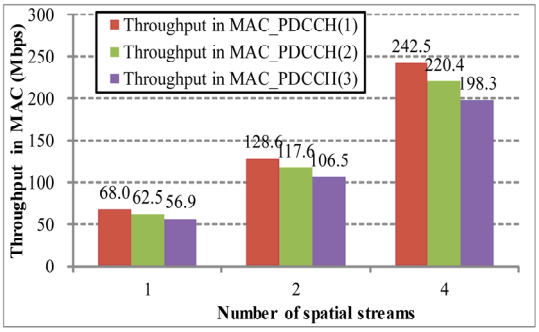

Figure 7. The downlink throughput of HeNB in MAC with 10% block error rate

3.2 The Throughput of 802.11n in MAC Layer

To evaluate the MAC throughput of 802.11n, the MAC layer protocol of 802.11, the Distributed Coordination Function (DCF) is introduced in [14]. Then the behavior of the MAC layer of 802.11 can be accurately analyzed using the Bianchi model [15] and the articles such as [16-17]. Based on the results in [18], the MAC throughput S of 802.11n can be written as

$$S = \frac{P_S P_{tr} E[P]}{(1-P_{tr})\sigma + P_{tr} P_S T_S + P_{tr}(1-P_S) T_C} \quad (8)$$

where T_S is the average time of the channel being sensed busy because of a successful transmission, and T_C is the average time of the channel being sensed busy by each station during a collision. σ, $E(P)$, P_S and P_{tr} denote the duration of an empty slot time, the average time to transfer a packet payload, the successful possibility to transmit a PPDU and the possibility to transmit a PPDU, respectively. New MAC layer features in 802.11n, such as block acknowledgment (BA) and Aggregate MAC Protocol Data Unit (A-MPDU) are designed to reduce MAC overhead in legacy DCF of 802.11. Thus, if we aggregate many MPDUs into one PLCP service data unit (PSDU) with a threshold size as large as 65535 bytes, instead of the 4096-byte limit in the traditional 802.11, the MAC throughput can increase tremendously if BA is applied to acknowledge the transmissions of all the MPDUs in this large PPDU. Here, the channel is assumed to be perfect. If the error rate is taken into account, the throughput of 802.11n can be obtained as

$$S = \frac{P_S (1-e) P_{tr} E[P]}{(1-P_{tr})\sigma + P_{tr} P_S (1-e) T_S + P_{tr}(1-P_S) T_C + (P_s T_C \sum_{i=1}^{M_C} i e^i)} \quad (9)$$

where e and M_C denote the error rate and the maximal re-transmission times for one frame transmission, respectively. If the evaluation parameters given in Table 2 and HT mixed PPDU format are employed, the throughput in MAC layer and the variables listed in (9) can be obtained as in Figure 8 and Table 3 by varying the number of spatial streams (1, 2 and 4) when the number of active stations, M

Table 2. The relevant parameters of 802.11n applied in Figure 3 and Equation (8)

Item	Parameters
Slot time (σ)	9 ìs
Propagation delay time (ä)	1 ìs
Coding rate (r_c)	5/6
Legacy Short Training Field (L-STF)	8 ìs
High Throughput SIGNAL field (HT-SIG)	8 ìs
PPDU formats	HT mixed format
Bandwidth	40 MHz
Number of spatial streams (N_{SS})	1, 2, 4 (N_{SS})
MCS index	31
Modulation	64-QAM
Legacy Long Training Field (L-LTF)	4 ìs
PSDU size (E[P])	65535 octets
Number of active stations (M)	1-10
PHY Data rate	150, 300, 600 Mbps

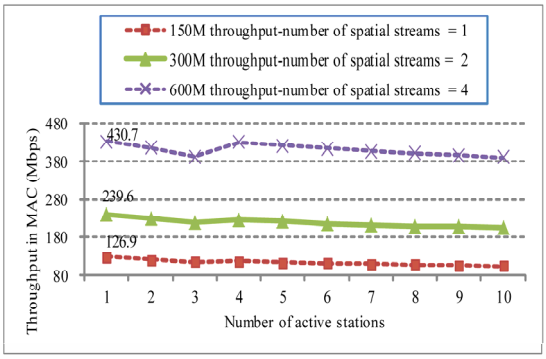

Figure 8. The MAC throughput of 802.11n with varying numbers of active stations and spatial streams with PPDU error rate=10%

ranges from 1 to 10 and the HT mixed PPDU format of 802.11n is used. The throughput shown in Figure 8 is based on the peak data rate in PHY, i.e. 150, 300 and 600 Mbps for the number of spatial streams 1, 2, and 4, respectively. When the number of active stations is greater than 1, the collision cost will increase and the throughput will decrease. However, when the number of stations reaches 4, the idle probability ($1-P_{tr}$) for one slot time is 0.704, which is much smaller than 0.882 for only one station; thus the maximal total MAC throughput, 430.7 Mbps, with the number of stations being 1 is similar to that of with 4, 430.3 Mbps for PHY data rate with 600 Mbps. This is also due to that fact that when the number of stations is larger than 4, the idle probability ($1-P_{tr}$) for one slot time does not fall sharply, as shown in Table 3. From Figure 4 and Table 3, we see the gap of peak total throughput between PHY (559 Mbps) with RS overheads and MAC (474.2 Mbps) layers in 802.11n with a perfect channel can be as large as 84.8 Mbps. Compared to HeNB, the distributed and easy approach adopted in the MAC of 802.11 pays a heavy penalty in performance loss especially when the frame size is not large.

Table 3. The MAC performance of 802.11n (MCS=31) with error rate=10% based on (9)

PHY Data rate=150 Mbps				
M	S	P_{tr}	P_S	Throughput (Mbps)
1	84.6%	11.8%	100.0%	126.9
2	80.8%	19.8%	94.5%	121.1
3	77.2%	25.5%	90.4%	115.8
4	77.4%	29.6%	87.3%	116.1
5	75.5%	32.7%	84.8%	113.3
6	74.0%	35.2%	82.8%	111.0
7	72.7%	37.2%	81.2%	109.0
8	71.6%	38.9%	79.8%	107.3
9	70.6%	40.4%	78.6%	105.9
10	69.7%	41.7%	77.5%	104.6
PHY Data rate=300 Mbps				
M	S	P_{tr}	P_S	Throughput (*Mbps*)
1	79.9%	11.8%	100.0%	239.6
2	76.5%	19.8%	94.5%	229.6
3	72.8%	25.5%	90.4%	218.5
4	75.4%	29.6%	87.3%	226.3
5	73.7%	32.7%	84.8%	221.0
6	72.2%	35.2%	82.8%	216.6
7	71.0%	37.2%	81.2%	212.9
8	69.9%	38.9%	79.8%	209.7
9	69.0%	40.4%	78.6%	206.9
10	68.1%	41.7%	77.5%	204.3
PHY Data rate=600 Mbps				
M	S	P_{tr}	P_S	Throughput (*Mbps*)
1	71.8%	11.8%	100.0%	430.7
2	69.2%	19.8%	94.5%	415.5
3	65.4%	25.5%	90.4%	392.5
4	71.7%	29.6%	87.3%	430.3
5	70.2%	32.7%	84.8%	420.9
6	68.8%	35.2%	82.8%	413.1
7	67.7%	37.2%	81.2%	406.4
8	66.8%	38.9%	79.8%	400.7
9	65.9%	40.4%	78.6%	395.6
10	65.1%	41.7%	77.5%	390.7

If we combine the results of Figures 6, Figure 7 and Figure 8, the comparison between 802.11n and HeNB with the maximal throughput with 10% block error rate and without error is illustrated in Figure 9.

4 The Co-Tier and Co-channel Interference Model of HeNB in LTE Networks and Hidden Terminal Effect in 802.11n

In fact, if a frequency band is allocated to two UEs connected to two neighboring HeNBs, the co-tier interference can be avoidable by assigning these resources in different sub-frames to the UEs if we assume the frame time for the nearby HeNBs is synchronized with each other. Even if the UEs are using the same frequency in the same sub-frame time, the *SINR* of the UEs might be high due to the long distance among the UEs resulting in low interference. After all, the uplink *SINR* of one UE i connected with HeNB h receiving interference from all the other UEs

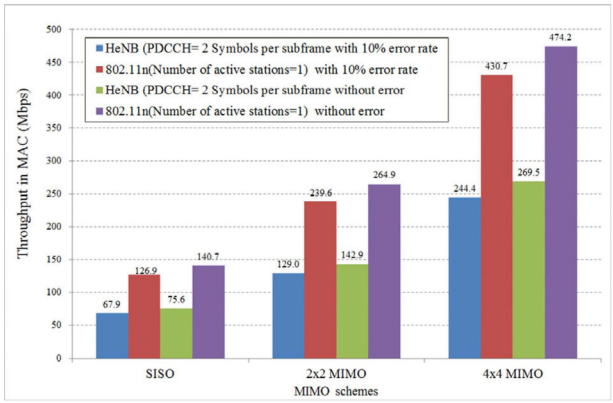

Figure 9. The comparison between 802.11n and HeNB with the maximal throughput in MAC with error rate=10% and without error

can be obtained by

$$SINR(i,h) = RSS(i,h)/(I_{total}+BN_0) = RSS(i,h)/(\sum_{\forall j\neq i} RSS(j,h)+BN_0). \quad \textbf{(10)}$$

where RSS (i, h), I_{total}, B and N_0 denote the received signal strength (RSS) of HeNB h from UE i, total interference from nearby UEs and HeNB, the spectrum bandwidth and thermal noise spectral density for the uplink, respectively.

If the power of HeNB and 802.11n is the same, the thermal noise of 802.11n is at least twice that of HeNB due to the fact that the employed bandwidth of 802.11n, 40 MHz is at least twice that of HeNB, 20 MHz in LTE networks. As a result, the *SNR* of HeNB can be at least 3 dB over that of 802.11n if the mixed-HT Mode is employed in 802.11n. Note that the received signal strength of UE for the downlink can be expressed in RSS (h, i) using this rule and can be given by

$$10\log_{10}(RSS(h,i))=10\log_{10}((P_h)\text{-}F(h)\text{-}PL(h,i)) \quad \textbf{(11)}$$

where P_h, $F(h)$ and $PL(h,i)$ denote the power of UE i, noise figure of HeNB i (expressed in dB) and the path loss from HeNB h *to* UE i in dB, respectively. In fact, the path loss involves Minimum Coupling Loss (MCL) defined as the minimum distance loss including antenna gain measured between antenna connectors [19]. The MCL between Base station (BS) and UE is used as a criterion for classification. Two classes are defined: Wide Area BS class and Local Area BS class. In this article, Local Area BS class with low MCL is assumed because of the indoor and the short distance characteristics of WLAN technology. In order to demonstrate the MCL, we use an APP called Wi-Fi analyzer installed on a UE, an Android smart phone, to detect the RSS from a Cisco wireless router (hotspot) named as linksys_Ting. The result is shown in Figure 10. The power issued from this hotspot is about 400 mW (26dBm), then the MCL, (26-(-35) =61dB) is obtained. Despite the fact that the estimation is based on the Wi-Fi, the study of [19] shows that the MCL is about 60dB in UMTS/IMT2000 systems; the exact value depends on the allocated spectrum. In fact, the path loss in an indoor environment for non-line-of-sight (*NLOS*) is really very hard to compute due to the complex block material.

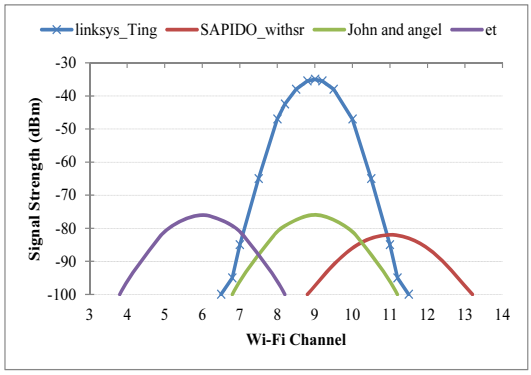

Figure 10. The signal strength received by UE in *dBm* varying with the Wi-Fi channel and the distance of UE to the hotspot, linkysys_Ting is less than 0.1m

The path loss for the dual-stripe model [1], UE inside the same apt stripe as HeNB can be given by

$$PL(i,h) = Max(20\log(d(i,h)) + 38.46 + 07d_{2D,indoor} + 18.3n^{(n+2)/(n+1)-0.46}, MCL) \quad \textbf{(12)}$$

where d (i, h), f_c and n denote the distance from UE i to HeNB h (or HeNB i to UE h) in meter, the frequency in *MHz* and the number of penetrated floors, respectively.

Note that $d_{2D,\ indoor}$ in (12) denotes the distance inside the house in meters. Specifically, the time domain for one UE is allocated in terms of 2 slot time, one sub-frame time. Hence, the total thermal noise is dependent on the frequency domain; it depends on how many RBs are allocated for this UE or HeNB. The total interference in the reception of HeNB and UE is really very complex, so we address the interference and *SINR* issues in the following subsection.

4.1 Co-tier, Co-channel Interference Model & SNR

If two UEs are using the same frequency band for uplink, the following topologies determine the path loss of these interferences. Note that the r, R and D denote the radius of the HeNB in meters, the distance of two HeNBs in meters and the distance of two neighboring cell edge in meters respectively as shown in Figure 11. If we fix the power, frequency spectrum effect, path loss from a sender to a receiver is a function of distance between them. Therefore, we can reduce the path loss in (12) to $PL(d)$ =20 $log(d)$ +C where d is the distance from a sender to a receiver and $C = 38.46 + 07d_{2D,indoor}$. Thus, C is a constant value if we fix $d2_{D,\ indoor}$ to 25 meters. Note that we assume all UEs are in the same floor, so the term $18.3n^{(n+2)/(n+1)-0.46}$

in (12) is ignored here. If the power *RSS* (*i*, *h*) and *RSS* (*j, h*) denote the received power from UE *i* and the interference from UE *j* respectively and if *RSS* (*j*, *h*) >>BN_0, and the power of UE *i*, P_i is the same with the power of UE *j*, P_j, the *SINR* of HeNB *h*, *SINR* (*h*) in dB can be given by

$$\begin{aligned} SINR(h) &\cong 10\log(RSS(i,h)/RSS(j,h)) \\ &= 10\log(RSS(i,h)) - 10\log(RSS(j,h)) \\ &= 10\log(P_i) - PL(d(i,h)) - (10\log(P_j) - PL(j,h)) \\ &= PL(d(j,h)) - PL(d(i,h)) \\ &= 20\log(d(j,h)) + C - (20\log(d(i,h)) + C) \\ &= 20\log(d(j,h)) - 20\log(d(i,h)) = 20\log(d(j,h)/d(i,h)). \end{aligned} \quad \textbf{(13)}$$

Figure 11(a) shows that the UEs of HeNB A and HeNB B are very close in the distance of *D* meters, so the uplink from UE A to HeNB A will interfere with the uplink of UE B to HeNB B and the same as the uplink of UE B to HeNB B. The rough *SINR* of HeNB A is equal to 20log(r/(r-D))= 0.294 based on (13) if the cell radius *r* and distance of two neighboring cell edges, *D* are set to 30 meters and 1 meter, respectively. The signal with low *SINR*, 0.294 can only carry little information per Hertz if the turbo coding and BSPK modulation are applied. On the contrary, the UEs of HeNB A and B have little interference with each other due to the long distance between them as shown in Figure 11(b). The received SINR of HeNB A is roughly equal to 20log ((3*r*-1/2*D*)/*r*) =15.5 if *r* and *D* are also set to 30 meters and 1 meter respectively as in Fig. 11(b). If the coding gain of turbo code in LTE is considered, the 16QAM even 64QAM can be applied. This phenomenon is well-known near-far effect, also called exposed terminal effect for 802.11. This truth also demonstrates that if a UE is very near to a HeNB, this HeNB can allocate all the uplink spectrum to this UE if FDD mode of LTE is assumed and the neighboring HeNB is not so near to this HeNB. The HeNB can allocate all its RBs according to this model; therefore the uplink throughput of UE can increase tremendously. This phenomenon can also be applied to the downlink scenario. The interference model is the same for the downlink as the situations as shown in Figure 11(a) and Figure 11(b). The situation in Figure 11(c) not like Figure 11(a) will not interfere with each other for the two UEs because there is a concrete wall blocking between them and the path loss of a concrete wall can be up to 20 dB [4]; hence, the HeNB A and B will not interfere or have little interference with each other. The interference shown in Figure 11(d) for the uplink is asymmetric; the received *SINR* of HeNB A, *SINR* (A) 20log(*r*/(*r*/2) = 6dB, but the received *SINR* of HeNB B, *SINR* (B) = 20log ((5*r*/2-*D*)/(*r*-*D*)) = 14.8 dB if we let *r*=30 and *D*=20. Hence, the interferences for the two HeNBs are asymmetric. The *SINR* of HeNB B will increase as the D grows larger so that the UE B can be more close to HeNB B and the near-far effect will grow stronger. This asymmetric characteristic can be applied in game theory for compromising the resource allocations for co-tier co-channel HeNBs [7-10]. The contradiction of resource allocations for the uplink of the two HeNBs as in Figure 11(d) will result in asymmetric penalty. It is interesting that the downlink interference as in Figure 11(d) is still asymmetric but the interference of UE B from HeNB A is larger than the interference of UE A from HeNB B but the interference from downlink is similar to that of uplink as in Figure 11(a)-11(c). We demonstrate all the received *SINR* and *SNR* of HeNB A and HeNB B of Figure 11 in Figure 12. In order to demonstrate the near-far effect, we vary the distance from UE A to HeNB A as in Figure 11(b) from 1 meter to 15 meters; the received *SNR* and *SINR* of HeNB A based on the parameters in Table 4 are shown in Figure 13. Figure 13 shows that if the distance is short to 1 meter, the *SINR* of HeNB A is as high as 40 even if there are interferences from UE B.

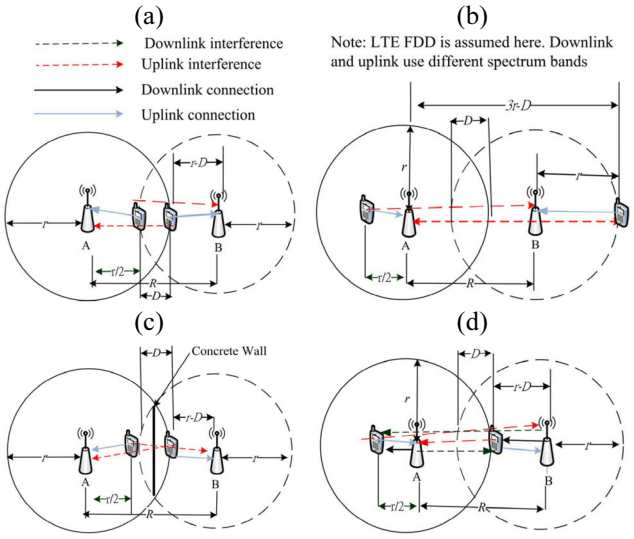

Figure 11. (a) Interference model for uplink; (b) Near-far effect and exposed terminal interference model for uplink; (c) Concrete wall interference model for uplink; (d) Asymmetric interference model for uplink and downlink

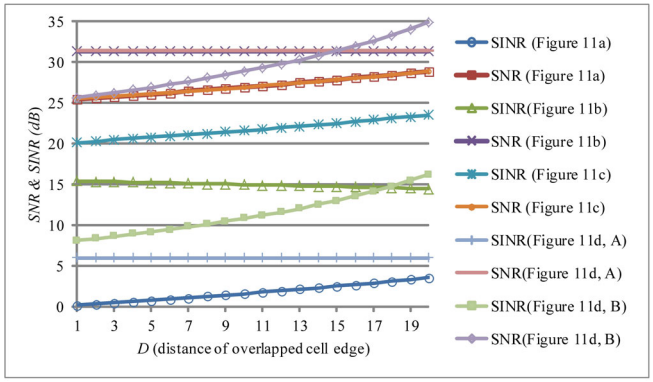

Figure 12. The received *SNR* & *SINR* at HeNB in Figure 11

Table 4. the parameters applied in Figure 1

Item	Parameter	Item	Parameter
r **(radius of coverage of HeNBs)**	30 m	***D***	Figure 11(a), Figure 11(c), Figure 11(d): 1m – 14m Figure 11(b): 1m
Power	23 dBm	***R***	$2r - D$ (59m -40m)
Frequency	2.0 GHz	**Wall path loss in Figure 11©**	20 dB
Bandwidth	10MHz	**Temperature**	300°K
Distance of UE A to HeNB A	Figure 11(a), Figure 11(c) and Figure 11(d): 15 *m* Figure 11(b): 1-15m	**Distance of UE B to HeNB B**	Figure 11(a), Figure 11(c), Figure 11(d): *r–D* Figure 11(b): 15m

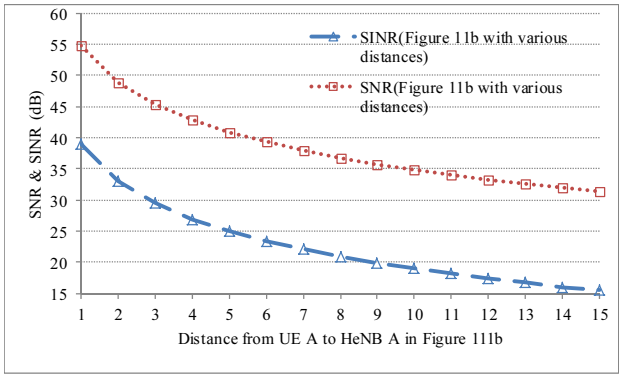

Figure 13. The received *SNR* & *SINR* from HeNB *A* in Figure 11(b) with varying distances from UE *A* to HeNB *A*

4.2 The Hidden Terminal Effect in 802.11n

The exposed and hidden terminal problems of 802.11 have been extensively researched by a lot of works such as [20-21], but the discussions of 802.11n for hidden terminal are rare. In general, the largest impact of 802.11n is its hidden terminal interference due to its distributed characteristics. In order to solve this hidden terminal effect, RTS/CTS mechanism proposed by the 802.11 standard is the most promising technique so far to our knowledge. However, when the PHY data rate of 802.11n can be up to 600 Mbps, the data time for common maximum frame size, 2304 Bytes is as short as 30 μs. Moreover in an OFDM system the data frame is carried by OFDM symbols, so the time to send the data frame is multiple times of one OFDM time; thus it needs 9 OFDM time, 32.4 μs to transmit this data frame. Hence, the overheads to carry the RTS/CTS frame are especially large when the data rate is high.

Note that the transmission of control frame must be very robust, so BPSK modulation in non-HT is adopted to transmit the control frames such as RTS, CTS and ACK frames. The data rate of BPSK is as low as 6 Mbps and the symbol time is extended to 4 us in non-HT mode; hence the time to transmit these control frames is 8 OFDM time, 32 μs because the sizes of RTS, CTS and ACK are 20 Bytes, 14 Bytes and 20 Bytes, respectively. The overheads for one frame transmission are illustrated as in Figure . Figure 14 shows that the MAC efficiency by employing the RTS/CTS to avoid the hidden terminal effect can be as low as 7.6 %; therefore the data rate in MAC is low to 45.3 Mbps despite the fact that the data rate in PHY can be as high as 600 Mbps. On the contrary, if the RTS/CTS mechanism is turned off, the MAC efficiency can be up to 13.6%; on the other words, the data rate in MAC can be double. It accounts for the fact that 802.11n will pay for the incredibly large penalty for the tremendous performance loss if the RTS/CTS mechanism is turned on. This penalty is no less than the co-tier, co-channel interference in HeNB of LTE networks as stated in the previous subsection.

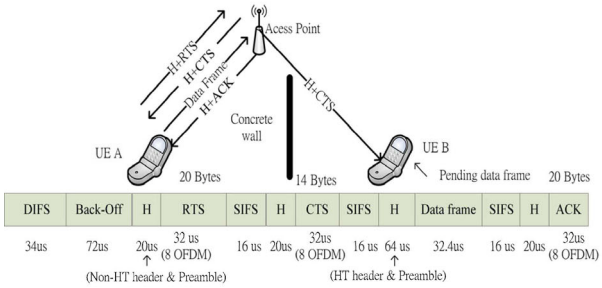

Figure 14. An illustration of the overheads of 802.11n to transmit a data frame when the mechanism of RTS/CTS is turned on

5 Discussion and Comparison of 802.11n and HeNB

In this article, based on the WLAN technologies, 802.11n and HeNB have been extensively studied in terms of PHY data rate, PHY overheads, MAC data rate, MAC overheads and interferences. Based on the results in the previous sections, it seems that HeNB will prevail over 802.11n with advantage in higher spectral efficiency in PHY layer. It is especially true when the frame size is not large. Therefore, 3GPP has launched the standardization hoping that LTE could be operated in unlicensed band. There have been two schemes, LTE unlicensed band (LTE-U) [22] and Licensed-Assisted Access (LAA) [23-24] proposed and discussed. Due to the low power limitation of

unlicensed band regulated by FCC, these bands are assumed to be applied in HeNB instead of eNB only generally. As mentioned above, our works can be a foundation to study LTE-U and LAA so that the benefit of LTE instead of 802.11 using some unlicensed bands can be calculated based on the model proposed in this article. In summary, we make a brief comparison between 802.11n and HeNB in Table 5. So far, the modulation scheme for LTE and LTE-A is limited to 64QAM. Therefore, the limit of spectrum efficiency for SISO is only 6bits/Hz per second. The future 5G networks [25] and the new generation of 802.11, 802.11ac [26-27] have set the 256QAM as the new modulation option as well as the 3GPP in Rel. 12 also supports 256 QAM as the modulation scheme for LTE-A in downlink. Moreover, its MIMO capability has been extended to 8x8 just like that of 802.11ac. Additionally, the bandwidth of LTE-A can be up to 100 MHz by the Carrier-Aggregation (CA) technique.

On the other hand, the bandwidth of 802.11ac can be up to 160 MHz through the Channel Bonding technique by the 5GHz spectrum with centimeter wavelengths. The bandwidth of 802.11ac can increase by 300% compared to that of HT mode of 802.11n. The Multi-User MIMO (MU-MIMO) has been proposed in 802.11ac as well as the HeNB for the future 5G network. If we assume all UEs are with infinite traffics ready to send and receive, and the number of UEs is greater than 8, the number of data streams to be sent and received simultaneously can be up to 8. It implies that the uplink capacity can increase by about 700% compared to that of SISO. After all, we apply the model listed above and make a performance comparison between 802.11ac and HeNB in the future 5G networks as in Figure 15(a), Figure 15(b) and Table 6. The MAC of 802.11ac is no longer limited to DCF only; instead MU-MIMO is also an option since the MIMO has been proposed about over one decade ago [8]. These estimations do not consider the new MAC behavior here. It is expected that it can also be listed as a future work.

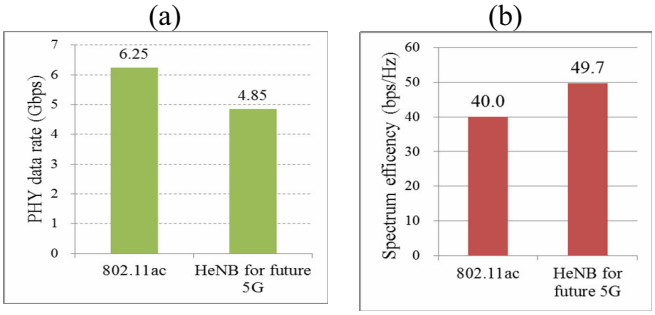

Figure 15. (a) PHY data rate comparison for 802.11ac and HeNB in the future 5G networks; (b) Spectrum efficiency comparison for 802.11ac and HeNB in the future 5G networks

6 Conclusion

The success or failure of the cloud computing in the

Table 5. Performance comparison between 802.11n and HeNB in LTE

Item		802.11n	HeNB
Peak data rate in PHY without considering PHY overheads		600 Mbps	373 Mbps
Percentage of PHY overheads	SISO	33.3% (1.5KB PSDU), 1.1% (64KB PSDU)	4.8%
	2x2MIMO	54.5.3% (1.5KB PSDU), 2.7% (64KB PSDU)	9.5%
	4x4MIMO	76.2% (1.5KB PSDU), 6.8% (64KB PSDU)	14.3%
Licensed/Unlicensed band		Unlicensed	Licensed
Available bandwidth		40 MHz/channel (HT) 20 MHz/channel (non-HT)	20 MHz (100 RBs)
Maximal spectral efficiency		15 bps/Hz	16 bps/Hz
Peak uplink throughput in MAC without error		140.7 Mbps (SISO) 264.7 Mbps (2x2 MIMO)	75.6 Mbps (SISO)
Peak downlink throughput in MAC with a perfect channel		474 Mbps (when the number of active UEs is 1)	248.9 Mbps to 294.1 Mbps
Hand-off		Needs scheduler of upper layer	Easy
Multi-user access capability		Extra penalty (collision cost, DIFS, back-off)	No or minor extra penalty
Cost		Low (small Fast Fourier Transform size)	High (large Fast Fourier Transform size)
Distributed or centralized		Distributed	Centralized
Interference		1. Hidden terminal problem 2. Collision problem	Co-tier/cross-tier co-channel interference
Coding scheme		LDPC &convolutional code	Turbo Code & convolutional code

Table 6. A brief performance comparison between 802.11ac and HeNB in the future 5G networks

Item	802.11ac	HeNB in the future 5G networks
MIMO scheme	8x8	8x8 (Massive MIMO has been proposed and discussed)
Maximal data rate in PHY without considering PHY overheads	6.25Gbps	4.85Gbps
Licensed/Unlicensed band	Unlicensed	Licensed
Available bandwidth	160 MHz by channel-bonding technique	100 MHz (500 RBs, the bandwidth might be expanded in the future 5G networks)
Maximal spectral efficiency	40 bps/Hz	49.7 bps/Hz
Hand-off	Needs scheduler of upper layer	Easy
Cost	Low (small Fast Fourier Transform size)	High (large Fast Fourier Transform size)
Distributed or centralized	Distributed (DCF) Centralized (MU-MIMO)	Centralized
Interference	Co-tier/cross-tier co-channel interference	DCF: 1. Hidden terminal problem 2. Collision problem MU-MIMO: co-channel interference
Coding scheme	LDPC & convolutional code	Turbo Code & convolutional code

future 5G networks depends on whether the wireless broadband is ubiquitous or not. The trend of frequency re-used and the appliance of OFDM and MIMO appearing in WLAN technology will prevail in the future to meet the requirements of this high data rate and high capacity for the future 5G networks. Due to the distributed characteristics of 802.11n, the spectrum efficiency of 802.11n is lower than that of HeNB especially when the frame aggregation is not applied for 802.11n. Furthermore, frame aggregation is only suitable for the traffics such as FTP with unbounded data to be sent but not sensitive to delay. Hence, the spectrum efficiency of 802.11 is indeed much lower that of HeNB in the general case not showing in this article. We owe it to the fact that the overheads of 802.11 PHY and MAC are really heavy. The RTS/CTS mechanism used to tackle the hidden terminal problem will let the overheads become much heavier. On the other hand, licensed spectrum for typical LTE is rare and precious; it motivates the upcoming LTE-U and LAA schemes to be proposed. A traffic type-ware resource sharing scheme also has been proposed based on cognitive radio networks [29]. The integration about the MAC or unlicensed spectrum sharing between these two systems will be a new future to attain the goals of 5G networks. This comparison model established in this article should be a good reference to attain this integration goal. In this article, we also establish an interference model taking advantages of the near far effect to mitigate the co-channel interference. It is expected that this effect can be a consideration factor of resource allocations negotiated between two neighboring HeNBs in the future protocol.

Acknowledgement

This work was supported by Ministry of Science and Technology of Taiwan under grant no. 105-2221-E-159-001. The author is also deeply grateful to Prof. Fang-Chang Kuo, Chih-Cheng Tseng, and Hwang-Cheng Wang of National Ilan University, as well as Prof. Chiapin Wang of National Taiwan Normal University. They provided valuable suggestions to the earlier conference version of this paper.

References

[1] 3GPP TR 36.814, *Further Advancements for E-UTRA Physical Layer Aspects*, v9.0.0 (Release 9), 2010.

[2] 3GPP TR 25.951, *Technical Specification Group Radio Access Network; FDD Base Station Classification* (Release 2000), V0.0.1 (2000-09), 2000.

[3] A. Molisch, A Generic Model for MIMO Wireless Propagation Channels in Macro and Microcells, *IEEE Trans. on Signal Processing*, Vol. 52, No. 1, pp. 61-71, January, 2004.

[4] T. S. Rappaport, W*ireless Communications: Principles and Practice*, Prentice Hall, 2002.

[5] V. Chandrasekhar, J. G. Andrews, T. Muharemovic, Z. Shen, A. Gatherer, Power Control in Two-tier Femtocell Networks, *IEEE Transaction on Wireless Communication*, Vol. 8, No. 8, pp. 4316-4328, August, 2009.

[6] R.-G. Cheng, S.-L. Tsao, 3GPP-WLAN Interworking Using a Novel Access Control Mechanism, *Journal of Internet Technology*, Vol. 6, No. 3 , pp. 261-272, July, 2005.

[7] D. T. Ngo, L. B. Le, L. N. Tho, E. Hossain, D. I. Kim, Distributed Interference Management in Two-tier CDMA HeNB Networks, *IEEE Transactions on Wireless Communications*, Vol. 11, No. 3, pp. 979-989, March, 2012.

[8] H. S. Jo, C. Mun, J. Moon, J. G. Yook, Self-optimized Coverage Coordination in HeNB Networks, *IEEE Transactions on Wireless Communications*, Vol. 9, No. 10, pp. 2977-2982, October, 2010.

[9] A. R. Elsherif, A. Ahmedin, Z. Ding, Adaptive Precoding for Femtocell Interference Mitigation, *IEEE ICC*, Ottawa, Canada, January, 2011, pp. 4632-4636.

[10] F. Pantisanoyz, M. Bennisz, W. Saad, R. Verdoney, M. Latva-ahoz, Coalition Formation Games for Femtocell Interference Management: A Recursive Core Approach, *IEEE Wireless Communications & Networking Conference*, Cancun, Mexico, 2011, pp. 1161-1166.

[11] P. Palanisamy, S. Nirmala, Downlink Interference Management in Femtocell Networks–A Comprehensive Study and Survey, *International Conference on Information Communication and Embedded Systems (ICICES)*, Tamilnadu, India, 2013.

[12] K. Aho, J. Puttonen, T. Henttonen, L. Dalsgaard, Channel Quality Indicator Preamble for Discontinuous Reception, *Proc. IEEE VTC-Spring*, Taipei, Taiwan, 2010, pp. 1-5.

[13] H. Holma, A. Toskala, *LTE for UMTS - OFDMA and SC-FDMA Based Radio Access*, Wiley, 2009.

[14] IEEE P802.11n/D3.0, *Draft Amendment to Standard: Wireless LAN Medium Access Control (MAC) and Physical Layer (PHY) Specifications: Enhancements for Higher Throughput*, 2007.

[15] G. Bianchi, Performance Analysis of the IEEE 802.11 Distributed Coordination Function, *IEEE Journal on Selected Areas in Communications*, Vol. 18, No. 3, pp. 535-547, March, 2000.

[16] K. C. Ting, H. C. Lee, F. Lai, A Scalable, High-Performance Grouping DCF for the MAC Layer Enhancement of 802.11n, *International Journal on Communication Networks and Distributed Systems* (IJCNDS), Vol. 7, Nos. 1/2, January, 2011, pp. 101-118.

[17] K. C. Ting, H. C. Wang, F. C. Kuo, C. C. Tseng, Decision of Mobile Devices Enabling HT and Non-HT MAC of 802.11n Based on the Consideration of Energy Efficiency, *Journal of Wireless Communications and Mobile Computing*, Vol. 14, No. 10, pp. 1007-1020, July, 2014.

[18] B. Jang, M. L. Sichitiu, IEEE 802.11 Saturation throughput Analysis in the Presence of Hidden Terminals, *IEEE/ACM Transactions on Networking*, Vol. 20, No. 2, pp. 557-570, April, 2012.

[19] P. Seidenberg, M. P. Althoff, E. Schulz, G. Herbster, M. Kottkamp, Statistics of the Minimum Coupling Loss in UMTS/IMT-2000 Reference Scenarios, *Gateway to 21st Century Communications Village. VTC 1999-Fall. IEEE VTS 50th Vehicular Technology Conference* (Cat. No.99CH36324), Amsterdam, Netherland, 1999, pp. 963-967.

[20] S. Khurana, A. Kahol, S. K. S. Gupta, P. K. Srimani, Performance Evaluation of Distributed Co-ordination Function for IEEE 802.11 Wireless LAN Protocol in Presence of Mobile and Hidden Terminals, *Proceedings of the 7th International Symposium on Modeling, Analysis and Simulation of Computer and Telecommunication Systems*, Piscataway, NJ, 1999, pp. 40-47.

[21] S. Khurana,A. Kahol, A. P. Jayasumana, Effect of Hidden Terminals on the Performance of IEEE 802.11 MAC protocol, *Proceedings of 23rd Annual Conference on Local Computer Networks*, Lowell, MA, pp. 12-20, 1998.

[22] Z. Li, C. Dong, A. Li, H. Wang, Traffic Offloading from LTE-U to WiFi: A Multi-objective Optimization Approach, *IEEE International Conference on Communication Systems (ICCS)*, Shenzhen, China, 2016, pp. 1-5.

[23] H. J. Kwon, J. Jeon, A. Bhorkar, Q. Ye, H. Harada, Y. Jiang, L. Liu, S. Nagata, B. L. Ng, T. Novlan, J. Oh, W. Yi, Licensed-Assisted Access to Unlicensed Spectrum in LTE Release 13, *A Revised Manuscript to IEEE Communications Magazine on LTE Evolution* on, April, 2016, http://arxiv.orf/ftp/arxiv/papers/1604/1604.08632.pdf.

[24] B. Chen, J. Chen, Y. Gao, J. Zhang, Coexistence of LTE-LAA and Wi-Fi on 5 GHz With Corresponding Deployment Scenarios: A Survey, *IEEE Communications Surveys & Tutorials*, Vol. 19, No. 1, pp. 7-32, March, 2017.

[25] L. Guo, Z. Ning, Q. Song, Y. Cui, Z. Chen, Toward Efficient 5G Transmission: SER Performance Analysis for Asynchronous Physical-layer Network Coding, *IEEE Access*, Vol. 4, pp. 5083-5097, November, 2016.

[26] T. T. T. Nguyen, L. Lanante, Y. Nagao, M. Kurosaki, H. Ochi, MU-MIMO Channel Emulator with Automatic Channel Sounding Feedback for IEEE 802.11ac, *IEEE Wireless Communications and Networking Conference*, Doha, Qatar, 2016, pp. 1838-1843.

[27] S. Abdallah, S. D. Blostein, Joint Rate Adaptation, Frame Aggregation and MIMO Mode Selection for IEEE 802.11ac, *IEEE Wireless Communications and Networking Conference*, Doha, Qatar, 2016.

[28] H. M. Wang, X. Q. Gao, B. Jiang, X. H. You, W. Hong, Efficient MIMO Channel Estimation Using Complementary Sequences, *IET Communications*, Vol. 1, No. 5, pp. 962-969, October, 2007.

[29] C. X. Mavromoustakis, G. Mastorakis, A. Bourdena, E. Pallis, Energy Efficient Resource Sharing Using a Traffic-oriented Routing Scheme for Cognitive Radio Networks, *IET Networks*, Vol. 3, No. 1, pp. 54-63, March, 2014.

Biography

Kuo-Chang Ting received his MS degree in computer science from the National Chung Cheng University, Taiwan in 1995. He received his PhD from EE, National Taiwan University in 2009. Now, he is an associate professor of Minghsin University of Science and Technology in Hsinchu, Taiwan.